SCIENTIFIC Publishing Limited

New Energy Exploitation and Application

https://ojs.ukscip.com/index.php/neea

Article

Performance Assessment of a Temperature-Based Model in Estimating GSR Across Different Latitudes of Cameroon

Edouard Mboumboue [1,2,*], Inoussah Moungnutou Mfetoum [3], Ahmed Ismail Arim [2] and Donatien Njomo [2]

[1] Department of Industrial Safety, Quality and Environment, National Advanced School of Mines and Petroleum Industries, University of Maroua, Maroua P.O. Box 46, Cameroon

[2] Environmental Energy Technologies Laboratory (EETL), Department of Physics, Faculty of Science, University of Yaounde 1, Yaounde P.O. Box 812, Cameroon

[3] Technology and Applied Sciences Laboratory, University Institute of Technology, University of Douala, Douala P.O. Box 8698, Cameroon

[*] Correspondence: edomboue@gmail.com

Received: 9 June 2025; **Revised:** 9 July 2025; **Accepted:** 21 July 2025; **Published:** 4 August 2025

Abstract: Among all climatic parameters, solar radiation is one, if not the most, involved in different applications (meteorology, agriculture, environment, etc.). However, due to economic constraints (especially in low-income countries like ours), it is not always measured. Over the years, several empirical correlations estimating global solar radiation (GSR) have been developed around the world by different authors. The objective of this study is to evaluate the performance and accuracy of a temperature-based model and to estimate the GSR received at four localities (Nanga Eboko, Ngaoundere, Tchollire and Maroua) in Cameroon. The studied model is that proposed by Hargreaves-Samani in 1982. It takes into account the latitude of the site and the daily minimum and maximum air temperatures. With commonly used statistical indicators (whose values are all within the acceptable range), the measured and estimated GSR values were compared and analyzed. According to the results, this model gives for the study area, a reasonable degree of good fitting and correlation between measurements and estimations. We also found that the further we move towards the north, the higher solar radiation is received and the performance of the model improves. Thus, from south to north, the country receives in average values, 4.6437 kWh m^{-2} d^{-1} at Nanga Eboko, 5.5667 kWh m^{-2} d^{-1} at Ngaoundere, 5.6968 kWh m^{-2} d^{-1} at Tchollire and 5.7936 kWh m^{-2} d^{-1} at Maroua. In case of missing data and taking into account the foregoing, we can consider the studied model as an accurate and useful tool in predicting GSR in the study area and similar geographical locations around the world.

Keywords: Cameroon; Empirical Model; GSR; Renewable Resources; Statistical Analysis

1. Introduction

Nowadays, energy (in all its forms) is proving to be the main driver of cultural, environmental, technological and socio-economic development around the world. It is to a country's economy what oxygen is to the human body. Like water and food, energy is essential for the life of a people or a nation. It has played a fundamental role in the development of civilizations. When poorly managed, its exploitation can be the source of several conflicts. The confiscation of access to energy resources has even been the cause of several wars between peoples [1]. During the

industrial revolution, easy access to abundant and cheap energy resources allowed faster and rapid socio-economic development. The discovery of electricity (the highly convenient form of energy), revolutionized the use of energy, and today it is almost impossible to imagine a modern home without electricity. However, despite this progress, a significant portion of the world's population still lacks access to energy. With the ever-increasing population boom and the legitimate desire to improve the quality of life, these energy needs are only increasing. If we add to this the scarcity of fossil fuel reserves, humanity is called upon to solve the thorny problem of continuing progress without consuming more energy. Energy is generally classified into two major groups, fossil fuels and renewable energies.

Renewable energies are those that are renewed by nature and whose cycling time is less than 100 years. Their renewal rhythm is higher than that of consumption [2]. Renewable energy systems use natural resources that are constantly renewed and generally less or non-polluting. The deployment of renewable energy technologies is essential for the future of the global economy. Renewable energies can make a significant contribution to the diversity and security of energy supply, and thus to socio-economic development. It can also address local and global environmental pollution. With low carbon content, particular attention has been paid to their potential to fight against global warming [3]. Renewable energy can be grouped into five main forms: solar, wind, hydro, geothermal, and biomass energy.

The exploitation of solar energy at a given site strongly depends on the solar radiation received there. Depending on the geographical position, this radiation varies from one place to another, which makes it necessary to have knowledge of this parameter for any new project. The GSR is the main input for different solar systems and the energy yield that may be expected from a solar power plant is very crucial for any investor. The amount of received GSR and its temporal distribution are the essential elements for a given solar application. Moreover, the development of any solar energy research program always begins with a study of solar radiation data [4]. GSR is essential for the sizing of solar installations, especially solar photovoltaic applications. However, there is a critical lack of measured data or, when it exists, it is not always reliable, due to cost, maintenance and calibration requirements. Even at stations where solar radiation is measured, there are several days where GSR data is missing or is outside the expected range due to equipment failure and other issues. For such stations where measured data is unavailable, the common practice is to estimate GSR (using empirical models) from other measured meteorological data such as sunshine duration, relative humidity, pressure, temperature, precipitation and many others [5,6]. Estimating GSR from widely available daily air temperature ranges (ΔT) offers a very good alternative to measured values. Xiaoying Liu et al. [7] have identified 16 temperature-based models, including modified versions of the Bristow and Campbell (B–C) and Hargreaves (Harg) models. Its results show an accuracy of the order of 4 to 7% between the original (B-C) model and the higher-performing modified (Harg) model, with a slight advantage for the (B-C) model. Djaman et al. [8], evaluated the performance and accuracy of about twenty solar radiation prediction methods with data from five meteorological stations and using the optimization procedure of the Excel solver in which the efficiency of Kling-Gupta is maximized. **Table 1** summarizes the main global solar radiation prediction models.

Table 1. A summary of the studied models.

Model No.	Equation	Coefficient(s)	Publication
1	$R_s = a \cdot (1 - \exp(-b \cdot \Delta T)) \cdot R_a$	a, b	Bristow and Campbell (1984) [9]
2	$R_s = 0.75 \cdot \left(1 - \exp\left(-b \cdot \Delta T^2\right)\right) \cdot R_a$	b	Meza and Varas (2000) [10]
3	$R_S = a \cdot \left(1 - \exp\left(-b \cdot \frac{\Delta T^c}{\Delta T_m}\right)\right) \cdot R_a$	a, b, c	Donatelli and Campbell (1998) [11]
4	$R_S = 0.75 \cdot \left(1 - \exp\left(-b \cdot \frac{\Delta T^2}{\Delta T_m}\right)\right) \cdot R_a$	b	Abraha and Savage (2008) [12]
5	$R_S = a \cdot \left(1 - \exp\left(-b \cdot \frac{\Delta T^c}{R_a}\right)\right) \cdot R_a$	a, b, c	Goodin et al. (1999) [13]
6	$R_S = 0.75 \cdot \left(1 - \exp\left(-b \cdot \frac{\Delta T^c}{Ra}\right)\right) \cdot R_a$	b	Weiss et al. (2001) [14]
7	$R_s = a \cdot \left(1 - \exp\left(-b \cdot f\left(T_{avg}\right) \cdot \Delta T^c\right)\right) \cdot R_a$ $f\left(T_{avg}\right) = 0.017 \exp\left(\exp\left(-0.053 \cdot T_{avg} \cdot \Delta T^C\right)\right)$	a, b, c	Donatelli and Campbell (1998) [11]
8	$R_s = 0.75 \cdot \left(1 - \exp\left(-b \cdot f\left(T_{avg}\right) \Delta T^2\right)\right) \cdot R_a$	b	Weiss et al. (2001) [14]
9	$R_s = a \cdot \left(1 - \exp\left(-b \cdot f\left(T_{avg}\right) \cdot \Delta T^2 \cdot g\left(T_{\min}\right)\right)\right) \cdot R_a$ $g\left(T_{min}\right) = \exp\left(\frac{T_{min}}{T_{nc}}\right)$	a, b, T_{nc}	Donatelli and Campbell (1998) [11]
10	$R_s = a \cdot \left(1 - \exp\left(-b \cdot f\left(T_{avg}\right) \cdot \Delta T^2 \cdot g\left(T_{\min}\right)\right)\right) \cdot R_a$	b, T_{nc}	Abraha and Savage (2008), Weiss et al. (2001) [12,14]

Table 1. *Cont.*

Model No.	Equation	Coefficient(s)	Publication
11	$R_s = a \cdot \sqrt{\Delta T} \cdot R_a$	a	Hargreaves model [15]
12	$R_s = a \cdot \left(1 + 2.7 \times 10^{-5} \cdot Alt\right) \sqrt{\Delta T} \cdot R_a$	a	Annandale et al. (2002) [16]
13	$R_s = \left(a \cdot \sqrt{\Delta T} + b\right) \cdot R_a$	a, b	Chen et al. (2004) [17]
14	$R_s = a \cdot \Delta T^b \cdot (1 + cP + dP^2) \cdot R_a$	a, b, c, d	De jong and Steward (1993) [18]
15	$R_s = a \cdot \sqrt{\Delta T} \cdot R_a + b$	a, b	Hunt et al. (1998) [19]
16	$R_s = a \cdot \sqrt{\Delta T} \cdot R_a + bT_{\max} + cP + dP^2 + e$	a, b, c, d, e	Hunt et al. (1998) [19]
17	$R_s = a \cdot \left(\sqrt{\frac{P}{101.3}}\right) \cdot \sqrt{\Delta T} \cdot R_a$ $P = 101.3 \cdot \left(\frac{293 - 0.0065z}{293}\right)^{5.26}$	a	Hargreaves and Samari (1982) [20] and Allen (1995) [21]
18	$R_s = a \cdot (b \cdot R_a T + c.T_{\max} \cdot T + d + T + e)$	a, b, c, d, e	Clemence (1992) [22]
19	$R_s = a + b \cdot R_a + c \cdot T$	a, b, c	Ertekin and Yaldiz (1999) [23]
20	$R_s = R_a \cdot \left(a \cdot \Delta T^{0.5} + b \cdot \Delta T^{1.5} + c \cdot \Delta T^{2.5}\right)$	a, b, c	Samani (2000) [24]
21	$R_s = R_a \cdot (a \cdot \ln(\Delta T) + b)$	a, b	Chen et al. (2004) [17]
22	$R_s = R_a \cdot (a + b \cdot T + c \cdot RH)$	a, b, c	El-Sebaii et al. (2009) [25]
23	$R_s = a \cdot R_a \cdot T^{0.25} + b$	a, b	Benghanem and Mellit (2014) [26]
24	$R_s = R_a \cdot (a + b \cdot T)\Delta T^c$	a, b, c	Hassan et al. (2016) [27]
25	$R_s = a \cdot R_a \cdot \exp\left(b \cdot \sqrt{\Delta T}\right)$	a, b	Rao model (2017) [7,8]
26	$R_s = R_a \left(a + b \cdot \Delta T + c \cdot \Delta T^2 + d \cdot \Delta T^3\right)$	a, b, c, d	Jahani et al. (2017) [28]
27	$R_s = R_a \left(a + b \cdot \Delta T + c \cdot \Delta T^{0.25} + d \cdot \Delta T^{0.5}\right)$	a, b, c, d	Fan et al. (2019) [29]
28	$R_s = \left(a \cdot \Delta T^{0.7} \cdot {R_a}^2 + b\right) \cdot R_a$	a, b	Nage (2018) [30]
29	$R_s = \left(a + b \cdot \sqrt{\Delta T} + c \cdot \ln(\Delta T)\right) \cdot R_a$	a, b, c	Nage (2018) [30]
30	$R_s = a \cdot \Delta T^b \cdot R_a$	a, b	Richardson model [7,8]
31	$R_s = (a + b \cdot \Delta T) \cdot R_a$	a, b	Djaman et al. (2020) [8]

$\Delta T = T_{max} - T_{min}$—diurnal range of air temperature (°C); $T = (T_{max} + T_{min})/2$ (°C); T_{avg}—daily average air temperature (°C); T_{max}—maximum daily air temperature (°C); T_{min}—minimum daily air temperature (°C); ΔT_m—monthly mean ΔT (°C); R_s—global solar radiation (MJ m^{-2} d^{-1}); R_a—extraterrestrial radiation (MJ m^{-2} d^{-1}); Alt—altitude (m); P—precipitation (mm); RH = mean relative humidity (%); Z = station altitude (m); a, b, c, d, e and T_{nc} are dimensionless empirical constants (to be determined during the calibration process).

Due to its geographical position (near the Equator), Cameroon receives abundant solar energy that can be usefully harnessed. The objective assigned to this article is to evaluate the performance and accuracy of a temperature-based model and to estimate the GSR received across four localities (with different latitudes) of Cameroon. The correlation developed is that suggested by Hargreaves & Samani. After the introductory section, Section 2 presents the sites, data and general methodology for conducting the study. Section 3 deals with the studied empirical model while Section 4 presents the main outcomes and discussions. The last section finally closes our study.

2. Sites, Data and Methodology

2.1. Study Area

Located in the western part of the Central Africa sub-region, Cameroon is positioned at the bottom of the Gulf of Guinea. It is situated between latitudes 1°40' and 13°05' North of the Equator and between longitudes 8°30' and 16°10' East of the Greenwich Meridian. The country covers an area of 475,650 km^2 of which 466,050 km^2 is land area and 9600 km^2 is sea area with 400 km of the coast [31]. The studied sites, indicated by an asterisk in the map of **Figure 1**, are, respectively, Nanga Eboko (in the Center region), Ngaoundere (Adamawa's region), Tchollire (North's region) and Maroua (Far-north's region). Based on the current administrative division of Cameroon, these sites were chosen according to their central position within the concerned regions. **Table 2** presents their geographical coordinates.

Table 2. Geographical location of the studied sites.

Site	Nanga Eboko	Ngaoundere	Tchollire	Maroua
Latitude (North)	4°40'	7°20'	8°23'	10°35'
Longitude (East)	12°22'	13°34'	14°10'	14°19'
Altitude (km)	9.98	19.61	5.71	19.85
Elevation (m)	582	911	1041	1314

Source: Google Earth Software.

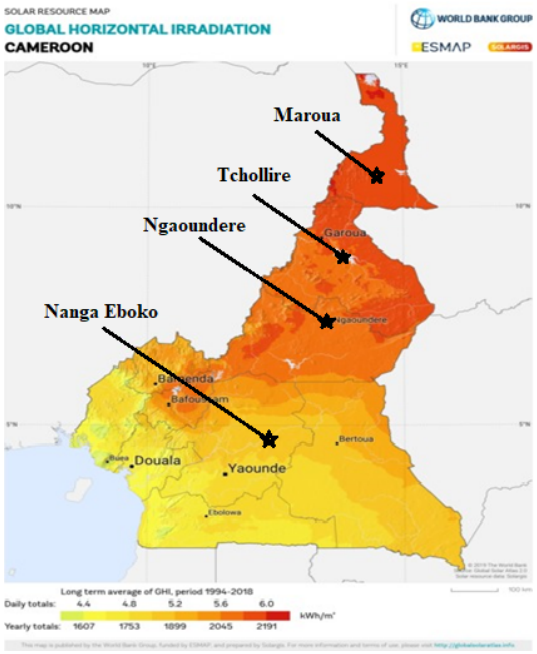

Figure 1. Solar map of Cameroon indicating solar energy potential (kWh/m^2) [32].

2.2. Data and Methods

Weather data, especially maximum and minimum air temperature in preparation for the highlighted model were obtained from the National Aeronautics and Space Administration (NASA) database [33]. It covers twenty-one years period (1984–2004). Moreover, ground measurements for a full year (1984) were obtained for the Nanga Eboko site. All these data were subjected to quality control procedures (including physical scanning, mass curve analysis, and use of box plots) to ensure that they are within the required logical and physical limits. Missing data were generated using the interpolation technique while spurious/erroneous data have simply been deleted. The flowchart of **Figure 2** summarizes the general methodology utilized in the study.

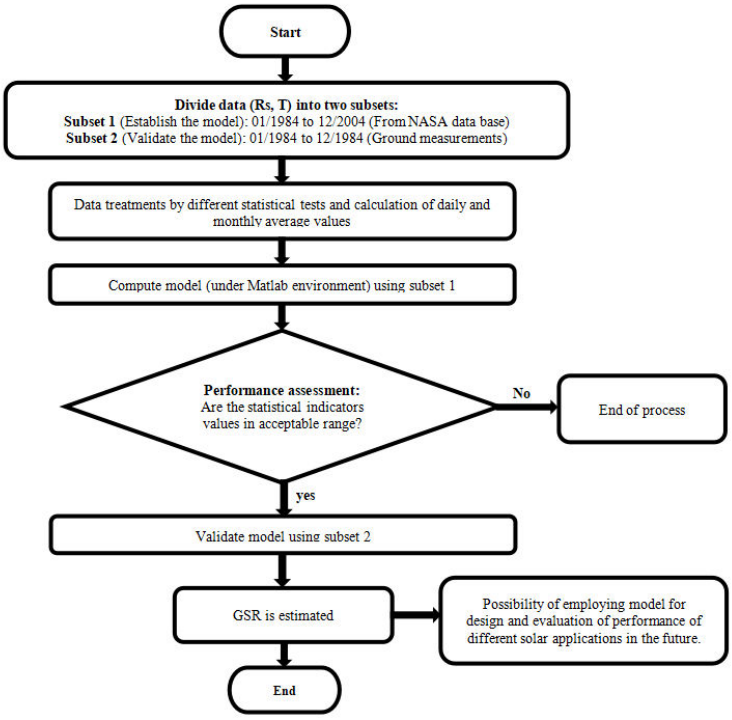

Figure 2. Flowchart describing the general procedure for determining GSR.

3. Empirical Correlation to Estimate GSR

According to several works [21,34–37], the monthly average of GSR on a horizontal surface is correlated with air temperature. In this paper, the model proposed by Hargreaves & Samani [21] is assessed across four localities. Hargreaves & Samani were the first authors to conduct a study using air temperature to estimate GSR by the following relations [20,38,39]:

$$R_s = aR_a\sqrt{(T_{\max} - T_{\min})} = aR_a\sqrt{\Delta T} \tag{1}$$

In this relation, Rs (in MJ m^{-2} d^{-1}) is the solar radiation received, Tmax and Tmin (in °C) are the daily maximum and minimum air temperature; Ra (in MJ m^{-2} d^{-1}) is the extraterrestrial radiation. Ra is a function of latitude and day of the year. 'a' is an empirical coefficient, its value is 0.16 for interior regions and 0.19 for coastal regions [36]. Ra is expressed by the relation 2 [38]:

$$R_a = \left(\frac{1440}{\pi}\right) \cdot Sc \cdot DF \cdot (\cos\varphi \cos\delta \sin\omega_s + \omega_s \sin\varphi \sin\delta) \tag{2}$$

Where Sc is the solar constant (1361.1 W/m^2 or 0.082 MJ m^{-2} min^{-1}) [40], DF is the eccentricity correction factor of the Earth's orbit, which can be calculated by the expression 3 [20]:

$$DF = 1.0 + 0.033\cos\left(2\pi\left(\frac{JulianDay}{360}\right)\right) \tag{3}$$

Where φ is the latitude of the site, it can be calculated by the relation:

$$\varphi = latitude \cdot \pi/180 \tag{4}$$

And δ is the solar declination, which can be expressed by the equation 5 [20]:

$$\delta = (23.45 \cdot \pi/180)\sin\left(2\pi\left(284 + \frac{JulianDay}{365}\right)\right) \tag{5}$$

ω_s (in degrees) is the sunrise hour angle. It is expressed by the relation 6 [39]:

$$\omega_s = \cos^{-1}(-\tan\varphi \tan\delta) \tag{6}$$

3.1. Statistical Analysis and Validation

For all considered sites, the accuracy of our estimations was tested by calculating the Root Mean Square Error (RMSE), the Mean Bias Error (MBE), the index of agreement (d) of Willmott, the coefficient of determination (R^2) and the coefficient of correlation (R). The RMSE (MJ m^{-2} d^{-1}), MBE (MJ m^{-2} d^{-1}), d(%), R^2 (%) and R are defined by the following relations [41–48]:

$$RMSE = \left[\frac{1}{n}\sum_{i=1}^{n}\left(R_{s_{meas}}(i) - R_{s_{est}}(i)\right)^2\right]^{\frac{1}{2}} \tag{7}$$

$$MBE = \frac{1}{n}\sum_{i=1}^{n}\left(R_{s_{est}}(i) - R_{s_{meas}}(i)\right) \tag{8}$$

$$d = 1 - \left[\frac{\sum_{i=1}^{n}\left(R_{s_{est}}(i) - R_{s_{meas}}(i)\right)^2}{\sum_{i=1}^{n}\left(\left|R_{s_{est}}(i) - \overline{R_{s_{meas}}(i)}\right| + \left|R_{s_{meas}}(i) - \overline{R_{s_{meas}}(i)}\right|\right)^2}\right] \tag{9}$$

$$R^2 = 1 - \frac{\sum_{i=1}^{n}\left(R_{s_{meas}}(i) - R_{s_{est}}(i)\right)^2}{\sum_{i=1}^{n}\left(R_{s_{meas}}(i)\right)^2} \tag{10}$$

$$R = \left[\frac{\sum_{i=1}^{n} \left(R_{s_{meas}}(i) - \overline{R_{s_{meas}}(i)} \right) \left(R_{s_{est}}(i) - \overline{R_{s_{est}}(i)} \right)}{\sqrt{\sum_{i=1}^{n} \left(R_{s_{meas}}(i) - \overline{R_{s_{meas}}(i)} \right)^2 \sum_{i=1}^{n} \left(R_{s_{est}}(i) - \overline{R_{s_{est}}(i)} \right)^2}} \right] \quad (11)$$

In equations (7–11), $R_{s_{meas}}(i)$ and $R_{s_{est}}(i)$ are respectively, the i^{th} measured and i^{th} estimated values of daily solar radiation while 'n' is the number of values.

The RMSE provides information on the short-term performance of the correlation by allowing a term-by-term comparison of the deviation between estimations and measurements. The values of the MBE represent the systematic error or bias; a positive value of MBE shows an overestimate, while a negative value shows an underestimate of the model. The smaller the value of error, the better the model's performance. For good accuracy and efficiency of the model, the values of (d) and R^2 should be closer to 1. The coefficient of correlation (R) is used to determine the linear relationship between measurements and estimations. It varies between −1 and 1.

4. Results and Discussions

For each location, the calculated values of GSR were compared to the measured ones. To find how good the model is, we performed various statistical tests like RMSE, MBE, d, R^2 and R. For sites where ground measurements are not available (Ngaoundere, Tchollire and Maroua), NASA data have been used to validate the model. **Table 3** below presents the main outcomes.

Table 3. Statistical analysis results.

Site	RMSE	MBE	d	R^2	R
Nanga Eboko	1.7801	−0.0932	0.6956	0.9997	0.5256
Ngaoundere	1.5502	0.0811	0.8051	0.9998	0.7320
Tchollire	1.2444	−0.0651	0.8162	0.9999	0.7677
Maroua	0.5932	−0.0310	0.9313	1.0000	0.8840

Globally, we observe a favorable and good agreement between measurements and estimations. We note from Table 2 that as the latitude of the site increases, the model becomes more accurate and performing. For every site, we can note that the higher the values of (d) and R^2 are, the lower the RMSE value becomes and vice versa, which indicates the good accuracy of the model. For Maroua site especially, we observe a perfect agreement (R^2 = 1, lowest RMSE and (d) closest to 1) between measurements and model estimates, meaning that the model is more adapted for this site. For Ngaoundere site, a slight overestimation is observed while for the rest, a slight underestimation is observed. This is probably caused by cloudy skies, which clouds, according to the seasons (rainy or dry), can sometimes suddenly appear and disappear. In the rainy season, normally, the amount of clouds is higher than in the dry season.

Equation (1) shows that the solar radiation (Rs) is proportional to the temperature range (ΔT). According to this relation, if ΔT increases (or decreases), so Rs increases (or decreases). **Figure 3** shows the yearly evolution of the temperature range (ΔT).

The monthly average values of ΔT observed are respectively, 5.6045 °C for Nanga Eboko, 8.3086 °C for Ngaoundere, 8.7809 °C for Tchollire and 9.0871 °C for Maroua. We can observe that the northern we move, the more accurate the model becomes (**Table 2** and **Table 3**). This result confirms the work of some authors [27–29] who assert that the temperature range ΔT is the main factor affecting the accuracy and performance of the temperature-based models. According to them, larger ΔT generally results in a better predictive accuracy, meaning that the temperature-based models are more applicable in areas with larger day-night temperature differences. It was observed in the study area that the less accurate results of fit and test were observed in sites with lower ΔT (Nanga Eboko especially). **Figure 4** and **Table 4** show, respectively, the graphical comparison of the measured and predicted values of GSR and the evolution of the temperature range (and GSR) with latitude.

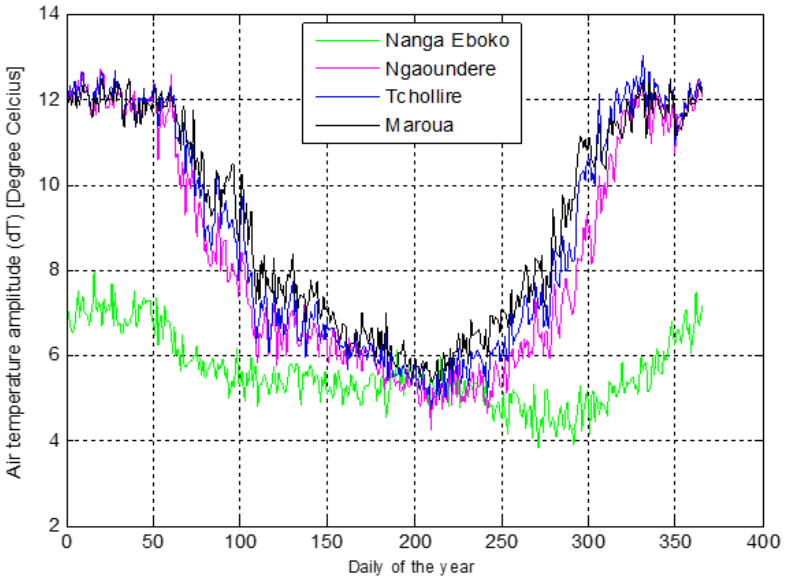

Figure 3. Yearly evolution of air temperature amplitude ΔT (Degree Celcius).

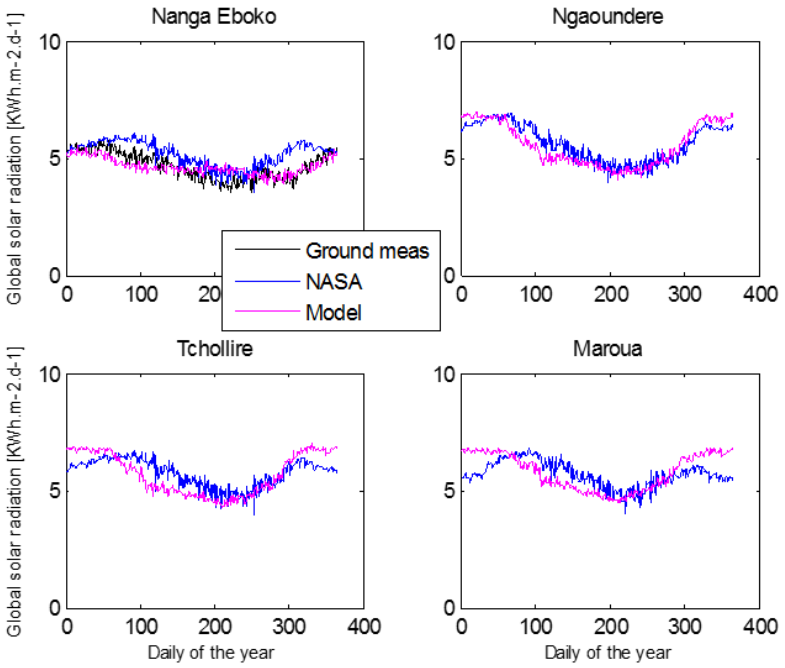

Figure 4. Yearly evolution of measured and predicted values of GSR (kWh m^{-2} d^{-1}).

Table 4. Evolution of the daily temperature range and GSR according to latitude.

Site	Latitude (North)	ΔT (°C)	GSR (kWh m^{-2} d^{-1})
Nanga Eboko	4°40’	5.6045	4.6437
Ngaoundere	7°20’	8.3086	5.5667
Tchollire	8°23’	8.7809	5.6968
Maroua	10°35’	9.0871	5.7936

Figure 5 shows the monthly evolution of GSR. It varies between 4.2241 kWh m^{-2} d^{-1} (Oct.) and 5.2137 kWh m^{-2} d^{-1} (Jan.) for Nanga Eboko; 4.4486 kWh m^{-2} d^{-1} (August) and 6.8107 kWh m^{-2} d^{-1} (Jan.) for Ngaoundere; 4.5481 kWh m^{-2} d^{-1} (Jul.) and 6.7956 kWh m^{-2} d^{-1} (Jan.) for Tchollire and 4.6776 kWh m^{-2} d^{-1} (Jul.) and 6.7258 kWh m^{-2} d^{-1} (Jan.) for Maroua. The most unfavorable months are, October for Nanga Eboko, August for Ngaoundere, and July for Tchollire and Maroua, while January is the sunniest month for all studied sites.

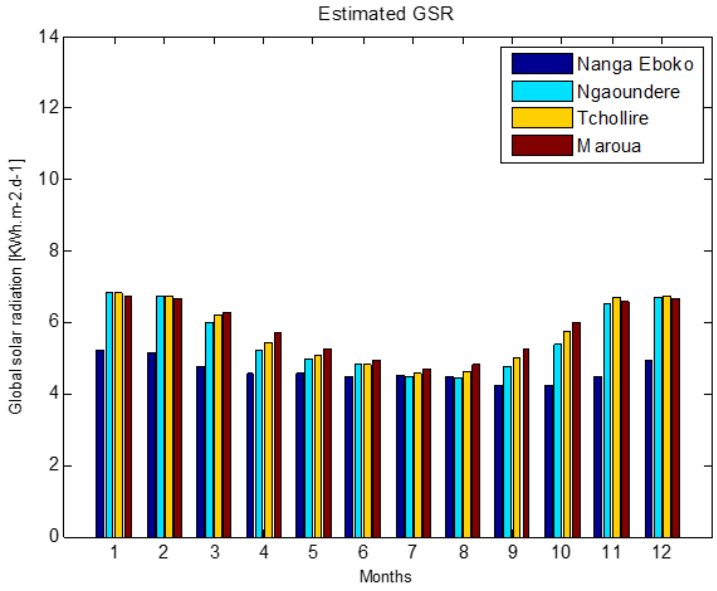

Figure 5. Monthly average of GSR (kWh m^{-2} d^{-1}).

As indicated in **Table 4**, the mean yearly GSR values are, 4.6437 kWh m^{-2} d^{-1} for Nanga Eboko; 5.5667 kWh m^{-2} d^{-1} for Ngaoundere; 5.6968 kWh m^{-2} d^{-1} for Tchollire and 5.7936 kWh m^{-2} d^{-1} for Maroua. In the national average, the solar radiation received in the country along the year is 5.4252 kWh m^{-2} d^{-1}. **Figure 6** shows the scatter plots of the measured and predicted values of GSR for the study area.

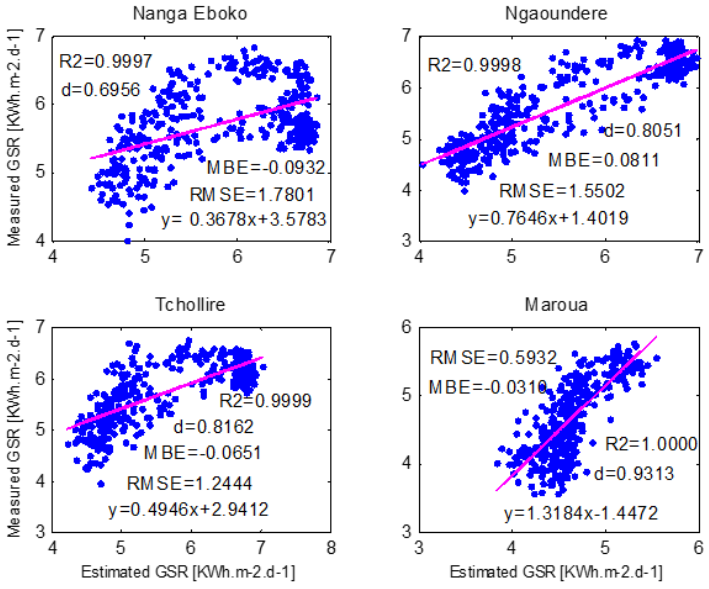

Figure 6. Scatter plots of predicted and measured values of GSR (KWh m^{-2} d^{-1}).

As in **Table 3**, it can also be seen from **Figure 6** that the performance of the model improves gradually with the increase of latitude. The minimum RMSE value of 0.5932 kWh m^{-2} d^{-1} was obtained in Maroua with high values of correlation coefficient (0.8840) and agreement index (0.9313) meaning that for this study area, the Hargreaves-Samani model performs well and gives the best estimation results for sites with high latitudes.

5. Conclusions

The knowledge of GSR at any site is vital for scientific, engineering, or environmental applications. In the absence of such data, reliable estimates can be made from easily available meteorological data such as cloudiness, sunshine, air temperature, or relative humidity along with extraterrestrial solar radiation using different models. In this study, the model proposed by Hargreaves-Samani (1982) was evaluated across four locations of Cameroon (with different latitudes) using the latitude and the daily minimum and maximum air temperature for the period 1984-2004. The performance and accuracy of this model were evaluated based on multiple statistical tests such as RMSE, MBE, d, R^2 and R. According to the results, this model gives for the study area, a reasonable degree of good fitting and correlation between the measured and estimated GSR. The coefficients of determination (R^2) are, 0.9997 for Nanga Eboko, 0.9998 for Ngaoundere, 0.9999 for Tchollire and 1.0000 for Maroua. We also found that the further we move towards the north, the higher solar radiation is received and the performance of the model improves. Thus, from south to north, the country receives, in average, 4.6437 kWh m^{-2} d^{-1} at Nanga Eboko, 5.5667 kWh m^{-2} d^{-1} at Ngaoundere, 5.6968 kWh m^{-2} d^{-1} at Tchollire and 5.7936 kWh m^{-2} d^{-1} at Maroua. In case of missing data and taking into account the above outcomes, we can consider the Hargreaves-Samani model as an accurate and useful model in predicting GSR in the study area and similar geographical locations around the world. For this reason, this work is, therefore, likely to stimulate and boost the development of solar energy applications across these areas.

List of symbols and acronyms:

a: Empirical coefficients of the model;
d: Index of agreement (%);
DF: Eccentricity correction factor of the Earth's orbit;
GSR: Global Solar Radiation (kwh m^{-2} d^{-1});
$R_{s_{\text{est}}}(i)$: i^{th} estimated values of daily Rs (kwh m^{-2} d^{-1});
$R_{s_{\text{meas}}}(i)$: i^{th} measured values of daily Rs (kwh m^{-2} d^{-1});
km: Kilometer;
m: meter;
MBE: Mean Bias Error (MJ m^{-2} d^{-1}/ kwh m^{-2} d^{-1});
n: Number of values;
NASA: National Aeronautics and Space Administration;
R: Correlation coefficient;
R^2: Coefficient of determination;
Ra: Extraterrestrial radiation (MJ m^{-2} d^{-1}/ KWh m^{-2} d^{-1});
RMSE: Root Mean Square Error (MJ m^{-2} d^{-1}/ kwh m^{-2} d^{-1});
Rs: Solar radiation (MJ m^{-2} d^{-1}/ KWh m^{-2} d^{-1});
Sc: Solar constant (1361.1 W/m^2);
Tavg: Daily average air temperature (°C);
Tmax: Daily maximum air temperature (°C);
Tmin: Daily minimum air temperature (°C);

Greek symbols

δ: solar declination (in degrees);
ϕ: Latitude of the site (in degrees);
ω_s: Sunrise hour angle (in degrees).

Author Contributions

Conceptualization, E.M. and I.M.M.; methodology, E.M. and A.I.A.; software, E.M.; validation, E.M., I.M.M. and A.I.A.; formal analysis, D.N.; investigation, E.M.; resources, A.I.A.; data curation, I.M.M.; writing—original draft preparation, E.M.; writing—review and editing, E.M.; visualization, I.M.M.; supervision, D.N.; project administration, D.N. All authors have read and agreed to the published version of the manuscript.

Funding

This work received no external funding.

Institutional Review Board Statement

Not applicable.

Informed Consent Statement

Not applicable.

Data Availability Statement

The data are accessible via the link of reference [33].

Conflicts of Interest

The authors declare no conflict of interest.

References

1. Bhattarai, U.; Maraseni, T.; Devkota, L.P.; Apan, A. Facilitating sustainable energy transition of Nepal: A best-fit model to prioritize influential socio-economic and climate perception factors on household energy behaviour. *Energy Sustain. Dev.* **2023**, *72*, 213–225.
2. Zekai, S. *Solar Energy Fundamentals and Modeling Techniques: Atmosphere, Environment, Climate Change and Renewable Energy*, 1st ed.; Springer: London, UK, 2008; pp. 1–X.
3. Fartash, K.; Ghorbani, A. From a promising technological niche to an established market niche: Solar photovoltaic niche formation in Iran. *Energy Sustain. Dev.* **2023**, *72*, 101–112.
4. Kumari, N.; Sharma,S.P.; Saksena, S.B.L. Comparison of different models for estimation of Global Solar Radiation in Jharkhand (India) Region. *Smart Grid Renew. Energy* **2013**, *4*, 348–352.
5. Kambezidis, H.D.; Psiloglou, B.E.; Karagiannis, D.; et al. Recent improvements of the Meteorological Radiation Model for solar irradiance estimates under all-sky conditions. *Renew. Energy* **2016**, *93*, 142–158.
6. Kambezidis, H.D.; et al. Meteorological Radiation Model (MRM v 6.1): Improvements in diffuse radiation estimates and new approach for implementation of cloud products. *Renew. Sustain. Energy Rev.* **2017**, *79*, 616–637.
7. Liu, X.; Mei, X.; Li, Y.; et al. Evaluation of temperature-based global solar radiation models in China. *Agric. For. Meteorol.* **2009**, *149*, 1433–1446.
8. Djaman, K.; Diop, L.; Koudahe, K.; et al. Evaluation of temperature-based solar radiation models and their impact on Penman-Monteith reference evapotranspiration in a semiarid climate. *Int. J. Hydrol.* **2020**, *4*, 84–95.
9. Bristow, K.L.; Campbell, G.S. On the relationship between incoming solar radiation and daily maximum and minimum temperature. *Agric. For. Meteorol.* **1984**, *31*, 159–166.
10. Meza, F.; Varas, E. Estimation of mean monthly solar global radiation as a function of temperature. *Agric. For. Meteorol.* **2000**, *100*, 231–241.
11. Donatelli, M.; Campbell, G.S. A simple model to estimate global solar radiation. In Proceedings of the 5th ESA Congress, Nitra, Slovak Republic, 28 June–2 July 1998.
12. Abraha, M.G.; Savage, M.J. Comparison of estimates of daily solar radiation from air temperature range for application in crop simulations. *Agric. For. Meteorol.* **2008**, *148*, 401–416.
13. Goodin, D.G.; Hutchinson, J.M.S.; Vanderlip, R.L.; et al. Estimating solar irradiance for crop modeling using daily air temperature data. *Agron. J.* **1999**, *91*, 845–851.

14. Weiss, A.; Hays, C.J.; Hu, Q.; et al. Incorporating bias error in calculating solar irradiance: implications for crop yield simulations. *Agron. J.* **2001**, *93*, 1321–1326.
15. Stanek, P.; Kuchar, L.; Otop, I. Estimation of diurnal total radiation based on meteorological variables in the period of plant vegetation in Poland. *ITM Web Conf.* **2018**, *23*, 00032. [CrossRef]
16. Annandale, J.G.; Jovanic, N.Z.; Benade, N.; et al. Software for missing data error analysis of Penman-Monteith reference evapotranspiration. *Irrig. Sci.* **2002**, *21*, 57–67.
17. Chen, R.S.; Ersi, K.; Yang, J.P.; et al. Validation of five global radiation models with measured daily data in China. *Energy Convers. Manage.* **2004**, *45*, 1759–1769.
18. De Jong, R.; Stewart, D.W. Estimating global solar radiation from common meteorological observations in western Canada. *Can. J. Plant Sci.* **1993**, *73*, 509–518.
19. Hunt, L.A.; Kucharb, L.; Swanton, C.J. Estimation of solar radiation for use in crop modelling. *Agric. For. Meteorol.* **1998**, *91*, 293–300.
20. Hargreaves, G.H.; Samani, Z.A. Estimating potential evapotranspiration. *J. Irrig. Drain. Div.* **1982**, *108*, 225–230.
21. Allen, R.G. Evaluation of Procedures for Estimating Mean Monthly Solar Radiation from Air Temperature. Technical Report, Food and Agriculture Organization (FAO), Rome, Italy, 1995.
22. Clemence B.S.E. An attempt at estimating solar radiation at South African sites which measure air temperature only. *S. Afr. J. Plant Soil.* **1992**, *9*, 40–42.
23. Ertekin C.; Yaldiz O. Estimation of monthly average daily global radiation on horizontal surface for Antalya, (Turkey). *Renew. Energy* **1999**, *17*, 95–102.
24. Samani Z. Estimating Solar Radiation and Evapotranspiration Using Minimum Climatological Data. *J. Irrig. Drain. Eng.* **2000**, *126*, 265–267.
25. El-Sebaii A.A.; Al-Ghamdi A.A.; Al-Hazmi F.S.; et al. Estimation of global solar radiation on horizontal surfaces in Jeddah, Saudi Arabia. *Energy Policy* **2009**, *37*, 3645–3649.
26. Benghanem M.; Mellit A. A simplified calibrated model for estimating daily global solar radiation in Madinah, Saudi Arabia. *Theor. Appl. Climatol.* **2014**, *115*, 197–205.
27. Hassan G.E.; Youssef M.E.; Mohamed Z.E.; et al. New temperature-based models for predicting global solar radiation. *Appl. Energy* **2016**, *179*, 437–450.
28. Jahani B.; Dinpashoh Y.; Raisi Nafchi A. Evaluation and development of empirical models for estimating daily solar radiation. *Renew. Sustain. Energy Rev.* **2017**, *73*, 878–891.
29. Fan J.; Wu L.; Zhang F.; et al. Evaluation and development of empirical models for estimating daily and monthly mean daily diffuse horizontal solar radiation for different climatic regions of China. *Renew Sustain. Energy Rev.* **2019**, *105*, 168–186.
30. Nage G.D. Estimation of Monthly Average Daily Solar Radiation from Meteorological Parameters: Sunshine Hours and Measured Temperature in Tepi, Ethiopia. *Int. J. Energy Environ. Sci.* **2018**, *3*, 19–26.
31. SIE_Cam. Système d'Information Energétique du Cameroun; Technical Report, 2010.
32. Solar resource maps & GIS data. Available online: https://solargis.com/resources/free-maps-and-gis-data?locality=cameroon (accessed on 8 July 2025).
33. NASA Prediction Of Worldwide Energy Resources (POWER). Available online: https://power.larc.nasa.gov (accessed on 1 December 2024).
34. Chandel, S.S.; Agarwal, R.K.; Pandey, A.N. New Correlation to Estimate Global Solar Radiation on Horizontal Surfaces using Sunshine Hour and Temperature Data for Indian Sites. *J. Sol. Energy Eng.* **2005**, *127*, 417–420.
35. Richardson, C.W. Weather Simulation for Crop Management Models. *Trans. ASAE* **1985**, *28*, 1602–1606.
36. Irwan, Y.M.; Daut, I.; Safwati, I.; et al. An Estimation of Solar Characteristic in Kelantan using Hargreaves Model. *Energy Procedia* **2013**, *36*, 473–478.
37. Li, H.; Cao, F.; Wang, X.; et al. A Temperature-Based Model for Estimating Monthly Average Daily Global Solar Radiation in China. *Sci. World* **2014**, *128754*, 1–9.
38. Lima, A.O.; Lyra, G.B.; Souza, J.L.; et al. Assessment of monthly global solar irradiation estimates using air temperature in different climates of the state of Rio de Janeiro, Southeastern Brazil. *SN Appl. Sci.* **2019**, *1*, 1002.
39. Bandyopadhyay, A.; Bhadra, A.; Raghuwanshi, N.S.; et al. Estimation of monthly solar radiation from measured air temperature extreme. *Agric. For. Meteorol.* **2008**, *148*, 1707–1718.
40. Gueymard, C.A. A reevaluation of the solar constant based on a 42-year total solar irradiance time series and a reconciliation of spaceborne observations. *J. Sol. Energy* **2018**, *168*, 2–9.
41. Gros, P. Use of the Linear Model: Basic Review–Validation Methods. Coastal Laboratories of Ifremer, Novem-

ber 2000. (in French)
42. Trahi, F. Prediction of Global Solar Radiation for the Tizi-Ouzou Region Using Artificial Neural Networks: Application for the Design of a Photovoltaic System to Supply the LAMPA Research Laboratory. Master's Thesis, Université Mouloud Mammeri de Tizi-Ouzou, Tizi-Ouzou, Algeria, 2011. (in French)
43. Confais, J.; Le Guen, M. Premiers pas en régression linéaire avec SAS. WP CES, 2007.
44. Willmott, C.J. On the validation of models. *Phys. Geogr.* **1981**, *2*, 184–194.
45. Willmott, C.J.; et al. A refined index of model performance. *Int. J. Climatol.* **2011**.
46. Besharat, F.; Dehghan, A.A.; Faghih, A.R. Empirical models for estimating global solar radiation: a review and case study. *Renew. Sustain. Energy Rev.* **2013**, *21*, 798–821.
47. El-Metwally, M. Sunshine and global solar radiation estimation at different sites in Egypt. *J. Atmos. Sol. Terr. Phys.* **2005**.
48. Almorox, J.; Hontoria, C. Global solar radiation estimation using sunshine duration in Spain. *Energy Convers. Manag.* **2004**.